BIOORGANIC CHEMISTRY 16, 133–148 (1988)

Conformation–Reactivity Relationships in Pyridoxal Model Systems: A Semiempirical Molecular Mechanics and MO–LCAO Investigation

A. M. VILLA, L. CASELLA,* AND P. FANTUCCI*

*Istituto di Chimica Farmaceutica e Tossicologica, V. le Abruzzi 42, I-20131 Milano, and *Dipartimento di Chimica Inorganica e Metallorganica, Centro CNR, Via Venezian 21, I-20133 Milano, Italy*

Received June 10, 1987

A preliminary investigation on the torsional hypersurface of the alanine Schiff bases with salicylaldehyde and pyridoxal was carried out by means of a van der Waals potential calculation. This allowed location of a few stable conformers, which were then subjected to a PCILO optimization. On the lowest energy conformer, an electrostatic molecular potential map was generated through a CNDO/2 calculation. Another pyridoxal model system, where the *N*-pyridoxylidene–alanine Schiff base is coordinated to a metal ion, was examined in order to check the relationship between the conformation at the amino acid α-carbon atom and the reactivity toward the C_α–H proton abstraction process. It has been found that the highest energy conformer containing a pseudoaxial C_α–H bond produces the most stable base adduct and carbanion species, in agreement with Dunathan's hypothesis. The potential biological significance of these results is discussed.

Vitamin B_6 is becoming more and more important in modern vitamin therapy of some very frequent and socially relevant diseases (*1*). Their still almost unknown pathogenesis as well as the variety of physiological events in which pyridoxal 5′-phosphate, the biochemically functional derivative of vitamin B_6, plays an essential role require a deeper understanding of all features of the enzymatic catalysis. Pyridoxal 5′-phosphate is the coenzyme for most enzymatic transformations involving amino acids (*2*). These reactions generally occur through the formation of an imine and labilization of one of the bonds to the amino acid α-carbon atom (*3*). An important feature of the enzymatic catalysis is its stereoelectronic control; this is achieved at the enzymatic active site by proper binding and conformational orientation of the substrate–cofactor imine complex (*4*). Model studies on pyridoxal Schiff bases of amino acids (**1**, see Chart 1) have been used to relate the NMR (*5*) and CD (*6*) spectra of the systems to the preferred conformation of the C_α–N bond. Similar stereochemical studies have been performed on the closely related Schiff bases derived from salicylaldehyde **2** (*7*) and on the metal chelates of these imines **3a** and **3b** (*8*), where the conformational mobility of the amino acid residue is largely restricted. Semiempirical conformational calculations have also appeared (*9*, *10*), although, in general, a detailed analysis of the conformation of the various bonds in this biochemically relevant family of compounds has never been reported.

0045-2068/88 $3.00

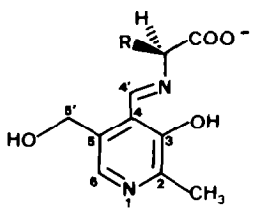

1

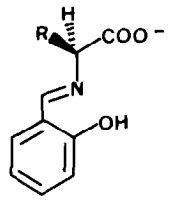

2

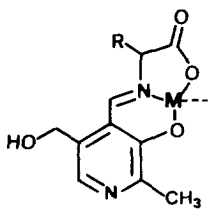

3a

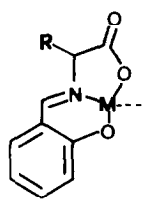

3b

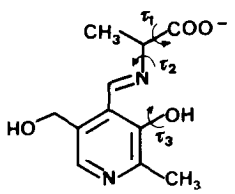

4b

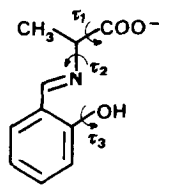

4a

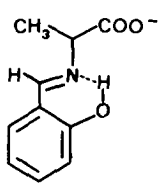

5

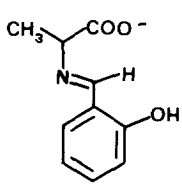

6

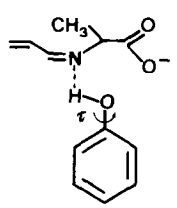

7

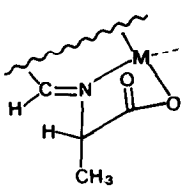

8a

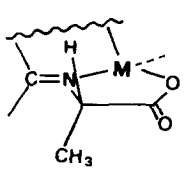

8b

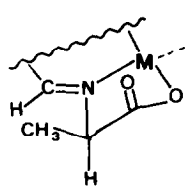

8c

CHART 1

This paper presents the results of a conformational study on systems of types **1–3**, with R=CH_3, carried out according to the PCILO method (*11*) in CNDO approximation (*12*). All internal rotation degrees of freedom were taken into account, leading to a fully investigated section of the energy hypersurface. A conformation–reactivity relationship emerging from the present study, with potential biological relevance, is also discussed.

COMPUTATIONAL METHOD

The present study has been carried out by means of the quantum mechanical method PCILO (*11*), using a modified version (*13*) of the QCPE program (*14*). Since the very large number of internal degrees of freedom prevents a full investigation of the energy hypersurface, only the potential energy variations associated with the internal rotations have been investigated, implicitly assuming a rigid-rotor approximation. In conformational studies, the fixed bond lengths and valence angles are usually taken from experimental X-ray data (if available) or are set equal to "standard" values. However, since the PCILO results concerning torsional motions can be influenced by the assumed fixed geometry of the molecular fragments involved, we preferred to optimize the bond lengths and valence angles directly connected with the rotation axis at a PCILO level. As a consequence, the resulting molecular geometry is of a mixed type, being derived partly from experimental or standard values and partly from PCILO optimum values. The procedure adopted may be justified if we consider that the values assigned to internal coordinates far from any rotation axis of interest cannot significantly influence the trend of the torsional energy, even if they do not coincide with their PCILO minimum values.

As it is well known, conformational studies are affected by very general limitations like those involved in locating the absolute and local minima on an energy surface of several dimensions. The present computational scheme adopts a conjugate-gradient type algorithm (*15*), and, for this reason, it is able to find the minimum energy point nearest to the starting point only. In principle, many different starting points should be chosen, in order to prove that the minimum found is the lowest one. But this procedure can be very expensive even when one is working with the PCILO method, which is known as the fastest approximate quantum chemical method for molecular energy calculations. Therefore we preferred to follow a different strategy. Starting from a fixed-valence molecular geometry (derived from X-ray data or standard values), the torsional hypersurface was fully investigated using thousands of random sampling points, the energy of which is evaluated by means of a simplified potential of the van der Waals type (*16*) for the 1–4 (nonbonded) interactions. This enables one to discard all conformations which are characterized by a high energy value due to short-range steric repulsions. The PCILO optimization of the torsional energy is then carried out starting from several of the lowest energy conformations previously found according to the van der Waals potential. When the absolute minimum is located with reasonable certainty, some of the most important bond distances and valence angles are

optimized, and a further search for the minimum on the torsional section of the surface leads to the final results. The present version of the computational program includes options for the random sampling of the surface using both the van der Waals (*16*) and PCILO potentials. Throughout this paper, the internal rotations τ_i are defined as τ(A–B–C–D), which is the counterclockwise rotation around B–C (view point C) which brings the C–B bond eclipsed with respect to the A–B bond.

RESULTS

The molecules we first investigated in the present study are the model compounds *N*-salicylidenealanine, **4a**, and *N*-pyridoxylidenealanine, **4b**. For both molecules three torsion angles have been considered (τ_1, τ_2, τ_3, see Chart 1).

Alanine–salicylaldehyde Schiff base ***4a***. For this model compound three different basic structures have been considered, namely the "*cis*"-isomer to the imine double bond, in which the side chain is forced to point toward the phenyl ring, and the structures **5** and **6** of Chart 1, which are two possible "*trans*"-isomers. Preliminary calculations showed that the *cis* structure lies at an energy much higher than the *trans* structures. Therefore the torsion energy surface of this isomer was not studied further. For the *trans*-conformers, the PCILO-optimized bond lengths and valence angles are reported in Table 1. The variation of the molecular energy accompanying the independent rotations τ_1, τ_2, and τ_3 around the minimum point

TABLE 1

PCILO-Optimized Geometry for **5**[a]

Carboxylate group		
Bond distance[b]	C—O	1.29
Bond angle	C_α—C=O	115.6
Bond angle	C_α—C—O^-	119.7
Torsion angle (τ_1)	$C_\alpha\hat{}^\beta COO^-$	203.4
Imine group		
Bond distance	C=N	1.30
Bond angle	C_1—C=N	120.4
Torsion angle (τ_2)	C=N$\hat{}^\beta$C	119.0
Phenolic group		
Bond distance	C_2—OH	1.38
Bond distance	O—H	1.09
Bond angle	C_2—O—H	107.4
Torsion angle (τ_3)	$C_2\hat{}^\beta$OH	180.0

[a] Numbering on carbon atoms refers to the phenyl nucleus of salicylaldehyde. Bond distances are in angstroms, angles in degrees.

[b] The two C—O distances were optimized under the constraint of equality in order to allow the maximum mesomeric effect through the PCILO perturbative charge transfer.

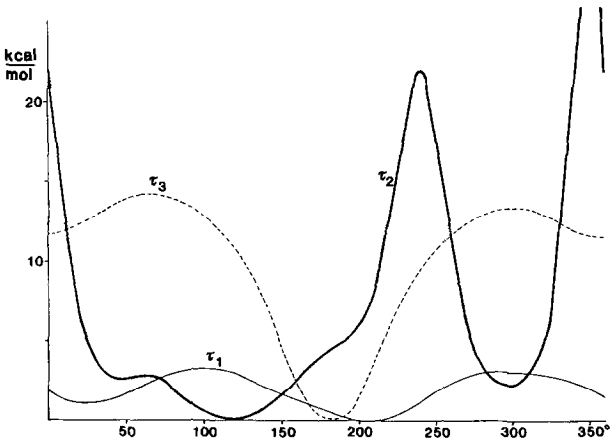

FIG. 1. Energy variations (kcal/mol) for the independent internal rotations τ_1, τ_2, and τ_3 for **6** (for the definition of these angles see text).

($\tau_1 = 203.4°$, $\tau_2 = 119.0°$, and $\tau_3 = 180.0°$ for **5** and $\tau_1 = 210.0°$, $\tau_2 = 120.0°$, and $\tau_3 = 180.0°$ for **6**) are displayed in Figs. 1 and 2. Conformer **5** is found to be more stable than **6** by about 23 kcal mol^{-1}, an extra stabilization which is certainly caused by the presence of the H bond in **5** between the phenolic proton and the N atom. An improved description of the H bond has been attempted by optimizing the ϕ–OH and ϕO–H distances and the ϕ–$\hat{O}$–H angle in the isomer **6**. The final results do not show any important change in the relative energy position of the two structures.

As for rotations τ_1 and τ_2, the behavior of the two isomers is very similar. Rotation τ_2 gives rise to two well-pronounced minima separated by energy barriers of 16–22 kcal mol^{-1} for $\tau_2 = 240°$ and 22–28 kcal mol^{-1} for $\tau_2 = 350°$. The two corresponding maxima are associated with a short-range interaction between the methyl and the carboxylate groups, respectively, and the imine proton. The isomers **5** and **6** behave very similarly also with regard to the energy changes accompanying the rotation τ_2. In fact, as expected, the τ_2 curve shows two minima separated by 180° and with relatively low energy difference (3–4 kcal mol^{-1}). The τ_3 angle, which controls the possibility of the H-bond formation in **5**, is associated with very different energy curves for the two isomers. Figure 2 shows that for compound **6**, the potential energy curve presents two maxima at $\tau_3 = 60$ and 290° lying at about 5 kcal mol^{-1} above the absolute minimum located in $\tau_3 = 180°$ (see Fig. 1). For compound **5**, the corresponding energy barriers occurring for $\tau_3 = 65°$ and $\tau_3 = 300°$ are as high as about 14 kcal mol^{-1}. Since the maxima present in the τ_3 curve correspond to a complete breaking of the H bond, one might conclude that the energy of the H bond in **5** is largely overestimated with respect to the values taken from experiments (*17*). However, in **5** the formation of an H bond is accompanied by the closure of a six-membered ring which certainly increases the stability of the conformation. In order to evaluate the two contributions (the pure H-bond formation and the six-atom ring effect), at least in an approximate way, PCILO calculations were carried out on the H-bonded adduct formed by a mole-

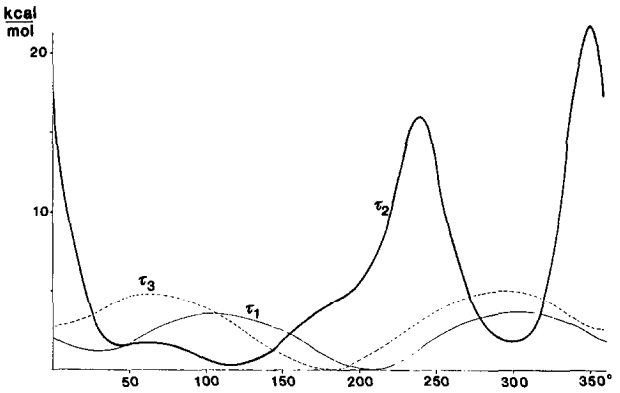

FIG. 2. Energy variations (kcal/mol) for the independent internal rotations τ_1, τ_2, and τ_3 for **5**.

cule of phenol with the Schiff base between alanine and acrolein, **7**. From the energy curve relative to the ϕ–OH rotation (Fig. 3), one can estimate that the pure H-bond contribution is of about 9 kcal mol^{-1}, a value falling within the range of known experimental data (*17*). As a consequence, it is possible to assign to the ring effect a contribution of about 5 kcal mol^{-1} to the total stability of conformer **5**.

Alanine–pyridoxal Schiff base ***4b***. Observations substantially analogous to those reported for **5** were made considering compound **4b**. The starting molecular geometry parameters taken from standard values have been subjected to a PCILO optimization procedure. The final results are reported in Table 2. The trend of the PCILO potential energy as a function of the independent rotations τ_1, τ_2, and τ_3 is plotted in Fig. 4; the variation of molecular energy is very similar to that accompanying the corresponding rotations in the salicylaldimine compound **5**. The further increase of the energy barrier for the rotation (τ_3) of the phenolic OH group (about 17 kcal mol^{-1} for $\tau_3 = 0°$) is due to a repulsive interaction between the phenolic hydrogen and the methyl group in position 2 of the pyridine ring, which is absent in **5**. The electron charge distribution of compound **1** has been examined in terms of Mulliken populations provided both by the PCILO method and by independent CNDO/2 calculations carried out in the PCILO minimum geometry. The agreement between the two sets of results is very satisfactory, despite the fact that the

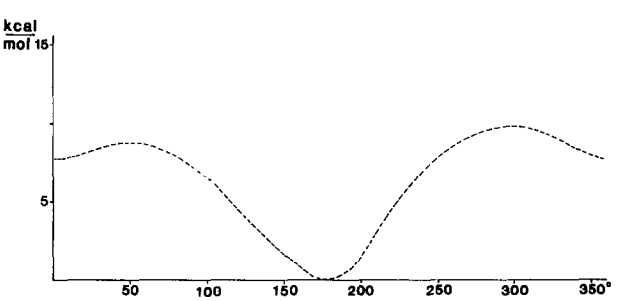

FIG. 3. Energy variations (kcal/mol) for the internal rotation τ for **7**.

TABLE 2

PCILO-Optimized Geometry for **4b**[a]

Carboxylate group		
Bond distance[b]	C—O	1.29
Bond angle	C_α—C=O	116.6
Bond angle	C_α—C—O^-	118.8
Torsion angle (τ_1)	C_α–β–COO^-	205.0
Imine group		
Bond distance	C=N	1.30
Bond angle	C—C=N	118.4
Torsion angle (τ_2)	C=N–β–C	119.0
Phenolic group		
Bond distance	C—OH	1.38
Bond distance	O—H	1.07
Bond angle	C—O—H	106.4
Torsion angle (τ_3)	C–β–OH	182.0
Other functions		
Bond distance	$C_{5'}$—OH	1.39
Bond distance	$C_{5'}$O—H	1.05
Bond angle	C_5—$C_{5'}$—O	110.8
Bond angle	$C_{5'}$—O—H	106.9
Torsion angle	C_5–β–$C_{5'}$OH	46.8
Torsion angle	$C_{5'}$–β–OH	179.3
Torsion angle	C_2–β–CH_3	57.9

[a] Numbering on carbon atoms refers to the pyridine nucleus of pyridoxal. Bond distances are in angstroms, angles in degrees.

[b] The two C—O distances were optimized under the constraint of equality in order to allow the maximum mesomeric effect through the PCILO perturbative charge transfer.

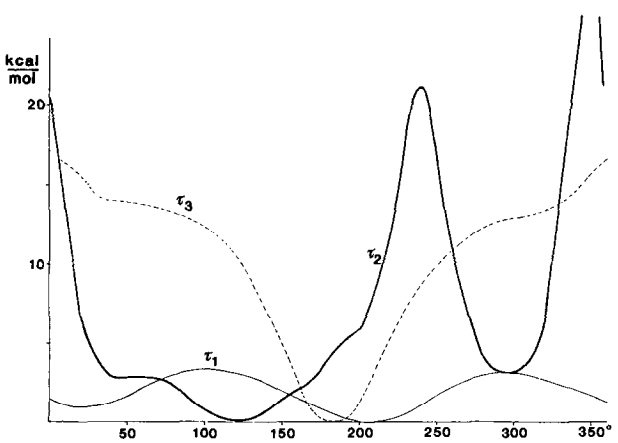

FIG. 4. Energy variations (kcal/mol) for the independent internal rotations τ_1, τ_2, and τ_3 for **4b**.

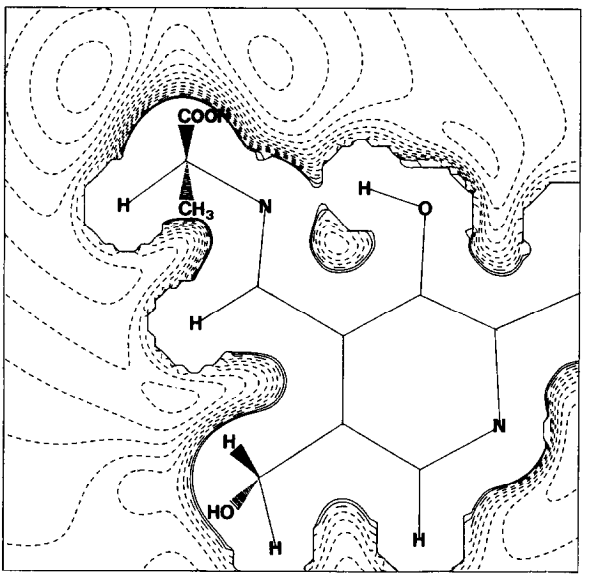

FIG. 5. Electrostatic molecular potential for **4b** (protonated form). The probe point charge moves around the molecule in the pyridoxylidene plane. The contours are drawn with dashed or full lines according to their attractive or repulsive character, respectively, and with an energy step of 10 kcal/mol.

PCILO total atomic charges do not result from a self-consistent procedure. This suggests that some molecular properties can be analyzed also within a SCF-CNDO procedure. In particular, in order to analyze the whole charge density of compound **1**, the "electrostatic molecular potential" (EMP), generated by a sampling positive point charge, has been computed from the CNDO wavefunction. The section of the EMP surface coincident with the pyridoxylidene plane is shown in Fig. 5. The drawing shows that the region around the C_α–H atom is strongly repulsive because of its "acid" character. The region is characterized by a sudden change in sign of the electrostatic interaction energy which presents the two lowest minima in the nearby regions around the carboxylic oxygen and the imine nitrogen atoms. Other minima of the EMP occur around the phenolic oxygen and pyridine nitrogen atoms. However, these two latter minima are much less deep than those of the C_α substituents. These results indicate the carboxylic function, especially in its anionic form, as the best candidate for interaction with positive polar sites of the enzyme. The "acidic" character of the C_α–H proton, as shown by the EMP map, is of some relevance with respect to the energetics involved in its mobilization, as discussed in the next section.

Alanine–pyridoxal Schiff base coordinated to a metal ion. It is well known that the conformational analysis of transition metal complexes is a difficult task because of the presence of *d* electrons which can hardly be described with a CNDO-type formalism (or its PCILO extension). In order to simplify the problem, we introduced the two following basic assumptions. First, the main effect of the metal

ion on the conformation of the alanine–pyridoxal Schiff base ligand is to form a chelate ring structure. Second, the metal center can be considered in an electronic situation to be close to the completely ionic M^{2+} state. In this context, we investigated the conformational characteristics of the model compound (*N*-pyridoxylidenealaninato)–metal(II) (compound **3** with R=CH_3), in which the metal ion is assumed to be Be^{2+} and a molecule of water occupies the fourth coordination position. While the geometry of the substituted pyridine moiety can be taken as the PCILO-optimized geometry for compound **1**, some problems may arise in regard to the assumption of the coordination geometry. Useful suggestions for this can be obtained from the known X-ray data of the two complexes *N*-salicylidenevalinatoaquacopper(II) (*18*) and *N*-salicylidenetyrosinatoaquacopper (II) (*19*). These complexes were chosen because they have the first coordination atoms lying in a plane, but differ significantly in the conformation of the amino acid chelate ring. The experimental data show that the dihedral angle between the plane containing the carboxylate group and that of the salicylidene system is as small as 13° in the tyrosine complex, while it is about 77° in the complex with the valine residue. Both these conformations have been considered in the calculations in order to investigate their possible influence on the chemical behavior of model compound **3a**. Hereafter, the nonplanar and the nearly planar conformations will be referred to as **8a** and **8b**, respectively (Chart I). The molecular geometry around the Be^{2+} ion of **8a** and **8b** has been optimized starting from the known data of the corresponding copper complexes. The results are listed in Table 3.

Since the C_α atom is the target for the action of the enzyme in many processes involving mobilization of the proton (*2, 3*), we carried out the optimization of the bond lengths and angles of the substituents on the amino acid C_α in order to have a better description of the electronic situation around this center. In the case of compound **8a**, the optimum values for the bond lengths and angles of the methyl carbon and the hydrogen atoms on C_α are very similar to those usually found for

TABLE 3

PCILO-Optimized Geometry for the Isomers **8a**, **8b**, **8x**, and **8c**[a]

		8a	**8b**	**8x**[b]	**8c**[c]
Bond distances	H_2O–Be	1.82	1.88	1.85	1.82
	COO–Be	1.70	1.71	1.71	1.70
	C_3O–Be	1.76	1.70	1.73	1.76
	N–Be	1.88	1.92	1.80	1.88
	C_α–CH_3	1.49	1.50	1.49	1.49
	C_α–H	1.13	1.14	1.14	1.13
Torsion angles	τ(OCC$_\alpha$N)	−76.6	13.3	−59.1	−76.6
	τ(CC$_\alpha$NBe)	−103.9	−122.3	−113.1	139.4
	τ(HC$_\alpha$NBe)	139.4	166.8	153.1	−103.9

[a] Bond distances are in angstroms, angles in degrees.
[b] Derived as weighted sum from the atomic coordinates of **8a** and **8b** (see text).
[c] Not optimized.

analogous compounds. The conformation of the methyl group on C_α is not very far from a pseudoaxial disposition. By contrast, in the case of the nearly planar conformation **8b**, both substituents to C_α occupy positions intermediate between pseudoaxial and pseudoequatorial. Also, the optimum C_α–H bond length is slightly longer than its common PCILO value (Table 3). The two conformers **8b** and **8a** differ in stability by not more than 5 kcal mol^{-1}, the former lying at lower energy, and therefore they can be easily converted into each other. Since the forms **8a** and **8b** were derived from experimental data relative to metal ion and amino acid residues different from those adopted in the present model calculations, neither **8a** nor **8b** is necessarily a local minima conformer on our PCILO hypersurface. In order to check this point, a few additional conformers i with atom coordinates collected in X_i intermediate between those of **8a** and **8b** (X_a and X_b, respectively) have been generated according to $X_i = (1 - \lambda)X_a + \lambda X_b$, with λ = 0.25, 0.5, and 0.75. For each value, the PCILO geometry optimization has been carried out for the C_α–H, C_α–CH_3, and N–$\hat{C}_\alpha$–CH_3 internal coordinates. We found that the species generated by $\lambda = 0.5$ is about 2 kcal mol^{-1} lower in energy than form **8b**. All the conformers considered show very similar C_α–H bond distances (in the range 1.13–1.14 Å) and total atomic charges.

Taking into account the limitations inherent to the present computational approach, one can conclude that none of the conformers examined is characterized by an enhanced molecular stability or electronic charge distribution which suggests an increased activation of the C_α–H bond toward the proton detachment process. In particular, the total charges, positive on the C_α–H proton and negative on the C_α atom, even confirming the EMP results relative to compound **1**, are not large enough to allow speculations about the proton mobilization and, consequently, the formation of a carbanion species. It is apparent that this is a highly energy-demanding process and that it must be promoted by a strong polarizing group approaching the C_α–H atom. In order to show the effect of such a polarizing group, we performed CNDO/2 calculations on conformers **8a** and **8b** and on the intermediate form generated by $\lambda = 0.5$ (**8x**), interacting with an NH_3 molecule or an OH^- ion. The complexes have been considered in their forms protonated at the pyridine nitrogen atom, since preliminary calculations carried out on the nonprotonated forms showed an energetically unfavorable C_α–H bond cleavage.

The reaction path of the basic group NH_3 or OH^- has been investigated at distances from the C_α–H proton ranging from 10 (assumed as a noninteraction distance) down to 1.008 (for NH_3) and 0.958 Å (for OH^-), which are the experimental N–H and O–H distances in ammonium salts and water, respectively (*20*). Further, the C_α–H bond has been "stretched," in order to find the best geometry for the supermolecule generated by the interaction between the base and the pyridoxal complex. Finally, the energy involved in the actual proton detachment process is evaluated increasing the relevant bond distance up to 10 Å.

Markedly different results have been obtained when the two base species are used. In the case of NH_3, one can clearly observe an enhanced polarization of the C–H bond, that is an increasing net charge on the proton and a negative net charge on carbon as the base approaches (see Table 4). The most stable supermolecule is characterized by an energy gain of about −3.5 kcal mol^{-1}, while the proton de-

TABLE 4

Energy Variations and Mulliken Population Data for the Interaction among Complexes **8a**, **8b**, **8x**, and NH_3

	Distance (Å)					
	N–H	C_α–H	ΔE (kcal/mol)	q_{NH_3}	q_H	q_C
8a	10.00	1.13	0.0	8.00	0.99	3.96
	2.00	1.13	−3.3	7.99	0.96	3.97
	1.01	10.00	175.9	7.27	0.73	4.19
8x	10.00	1.14	0.0	8.00	0.98	3.96
	2.00	1.14	−3.4	7.99	0.96	3.98
	1.01	10.00	172.5	7.27	0.73	4.21
8b	10.00	1.14	0.0	8.00	0.98	3.96
	2.00	1.14	−3.5	7.99	0.95	3.98
	1.01	10.00	172.9	7.27	0.73	4.24

tachment process, leading to a NH_4^+ ion and the C_α carbanion species, requires a high energy expense (more than 170 kcal mol^{-1}). In the case where the reacting moiety is a much stronger base, i.e., OH^-, the formation of the supermolecule gives rise to an energy gain as high as 160–165 kcal mol^{-1}, while the further step, involving detachment of the proton, requires an energy expense of 27, 23, and 21 kcal mol^{-1} for conformers **8a**, **8x**, and **8b**, respectively (see Table 5). Therefore, for all three conformers, the proton detachment process is very favorable from an energetic point of view.

An additional structure for compound **3a** (**8c**) has been generated from structure **8a** by epimerization at the C_α atom, thus forcing the C_α–H proton into a pseudoax-

TABLE 5

Energy Variations and Mulliken Population Data for the Interaction among Complexes **8a**, **8b**, **8x**, **8c**, and OH^-

	Distance (Å)					
	O–H	C_α–H	ΔE (kcal/mol)	q_{OH^-}	q_H	q_C
8a	10.00	1.13	0.0	8.00	0.99	3.96
	1.00	1.30	−165.1	7.16	0.80	3.99
	0.96	10.00	−138.3	7.15	0.85	4.18
8x	10.00	1.14	0.0	8.00	0.98	3.96
	1.00	1.30	−164.4	7.22	0.80	4.06
	0.96	10.00	−141.5	7.15	0.85	4.19
8b	10.00	1.14	0.0	8.00	0.98	3.96
	1.00	1.30	−160.8	7.28	0.77	4.13
	0.96	10.00	−140.9	7.15	0.85	4.23
8c	10.00	1.13	0.0	8.00	0.98	3.96
	1.00	1.30	−183.4	7.22	0.79	4.05
	0.96	10.00	−159.0	7.15	0.85	4.14

ial arrangement. According to the value for the CNDO/2 total energy of **8c**, this lies at about 17 kcal mol^{-1} above the most stable conformer **8x**. However, **8c** seems to be highly active with respect to the reaction with OH^-, giving rise to a supermolecule and to a carbanion species more stable than the corresponding derivatives obtained from **8a**, **8b**, and **8x**. This suggests that the axial disposition for the C_α–H bond significantly increases its reactivity toward proton-mobilizing agents.

DISCUSSION

The conformational calculations performed on the imines **1** and **2** show that the most stable conformers about the C_α–N bond occupy a broad range of structures minimizing the interaction between the substituent to the α-carbon atom and the azomethine proton of the Schiff base. Thus, the most stable conformations contain the C_α–H proton in the vicinity of the imine proton. These results are in agreement with previous NMR (*5*) and CD (*6*) spectral studies. Intramolecular hydrogen bonding between the phenolic proton and the imine nitrogen atom markedly stabilizes one of the *trans*-isomers to the imine double bond, **5** (that with a *cis* conformation of the C_4–$C_{4'}$ bond). By contrast, we find that the carboxylate oxygen atoms cannot reach a position to give significant bonding interaction with the phenolic proton, as is often assumed (*3*). Comparison with the behavior of the acrolein Schiff base **7** shows that separate contributions from pure H-bond formation and six-membered ring formation determine the high stability of hydrogen-bonding interactions in the imines **1** and **2**.

One main purpose of the present investigation was to gain some understanding of the relationships between conformation and reactivity in systems related to vitamin B_6-catalyzed reactions. Stereoelectronic effects are known to be very important in determining the specificity with which enzymatic reactions occur. In the case of pyridoxal-mediated reactions this is usually achieved by selection of the bond to be broken at the α-carbon atom of the amino acid residue. It is generally thought that proper conformational orientation of the substrate–cofactor imine at the active site is accomplished by three-point binding to the apoenzyme, through the pyridine nitrogen and phosphate group of the cofactor and a distal group on the substrate, possibly the carboxylate group when amino acids with nonpolar side chains are involved. In 1966 Dunathan proposed that the bond to be broken in the substrate–cofactor imine had to be oriented perpendicularly to the plane of the extended conjugated π-system for an easy breaking process (*21*). Since then this proposal has become the routine working hypothesis to interpret the stereochemical course of pyridoxal phosphate enzyme reactions (*4*) (see, e.g., Refs. (*22–25*)). In order to test Dunathan's hypothesis we chose to investigate conformation–reactivity relationships in the model systems represented by metal chelates **3a**. These were selected for their ability to reproduce to some extent enzymatic processes that are completely inhibited in the absence of metal ions (*3*, *26–28*). The presence of two adjacent chelate rings has the additional advantage, from the computational point of view, of imposing a drastic reduction in the

conformational mobility of the ligand with respect to the corresponding metal free systems of type **1**.

The simplest process to be studied for systems of type **3a** is the cleavage of the C_α–H bond, which represents the preliminary step in a variety of enzymatic reactions undergone by amino acids during metabolism, such as racemization, transamination, β-elimination, γ-elimination, and retroaldolization (*2*). The systems of type **3a** are less suited to study other processes, such as decarboxylation, since they contain the carboxylate group in a blocked conformation. The relationship between labilization, and then cleavage, of the C_α–H bond and its conformational arrangement within the chelate ring of the amino acid residue was thus investigated. The three limiting structures **8a**–**8c** were considered, together with a fourth optimized structure **8x** intermediate between **8a** and **8b**. We can refer to structures **8b**, **8a**, and **8c** as those containing an approximately planar chelate ring, a pseudoequatorial C_α–H bond, and a pseudoaxial C_α–H bond, respectively. The detachment of the proton was simulated by the approach of a suitable base along the C_α–H bond direction.

Two general aspects of the reactivity emerge from the calculations independent of the structure considered: (i) the effect of protonation of the pyridine ring nitrogen of the pyridoxal residue, and (ii) the nature of the approaching base. Protonation of the pyridine ring of the pyridoxal residue appears a necessary requisite for an easy C_α–H bond cleavage. But the nature of the base is important as well, since with a weak base such as NH_3 the bond rupture requires a large energy expense (150–180 kcal mol^{-1}) in any case. The enhancement of reactivity on protonation of the pyridine ring of pyridoxal has been recognized in model systems (*8, 26*) and is probably largely responsible for the higher reactivity of the pyridoxal metal chelates **3a** with respect to their salicylaldehyde analogs **3b** (*26–28*), e.g., in racemization reactions, since the pyridine ring is significantly protonated in protic, neutral media (*29*). This effect has biological relevance, since it is usually assumed that the pyridine ring of pyridoxal phosphate at the enzyme active site is also protonated at physiological pH (*4*). The effect of the nature of the base used for C_α–H proton abstraction is also marked well beyond the approximation of the computational method and indicates that a strong base is required for an easy C_α–H bond-breaking process. This result may also have biological relevance, since the energy required for C_α–H proton detachment by the base NH_3 is so high that it seems unlikely that an amino group like that on a lysine side chain, or perhaps a histidine imidazole group, can function as the proton-abstracting species in the natural systems even under the most favorable conditions. In this respect it should be noted that the polarizing effect produced on the imine ligand by the positive charge of the metal ion in the chelate **3a** is probably stronger than that produced at the enzyme active site on binding of the substrate–cofactor complex, i.e., the phosphate ester derivative of **1**. In other words, the C_α–H proton abstraction process in model system **3a** with the pyridine ring protonated may represent an optimum condition from the point of view of the activation of the substrate by its environment.

The energetics involved in the C_α–H proton abstraction by the base OH^- for the structures **8a**–**8c** gives an opportunity to discuss conformation–reactivity relation-

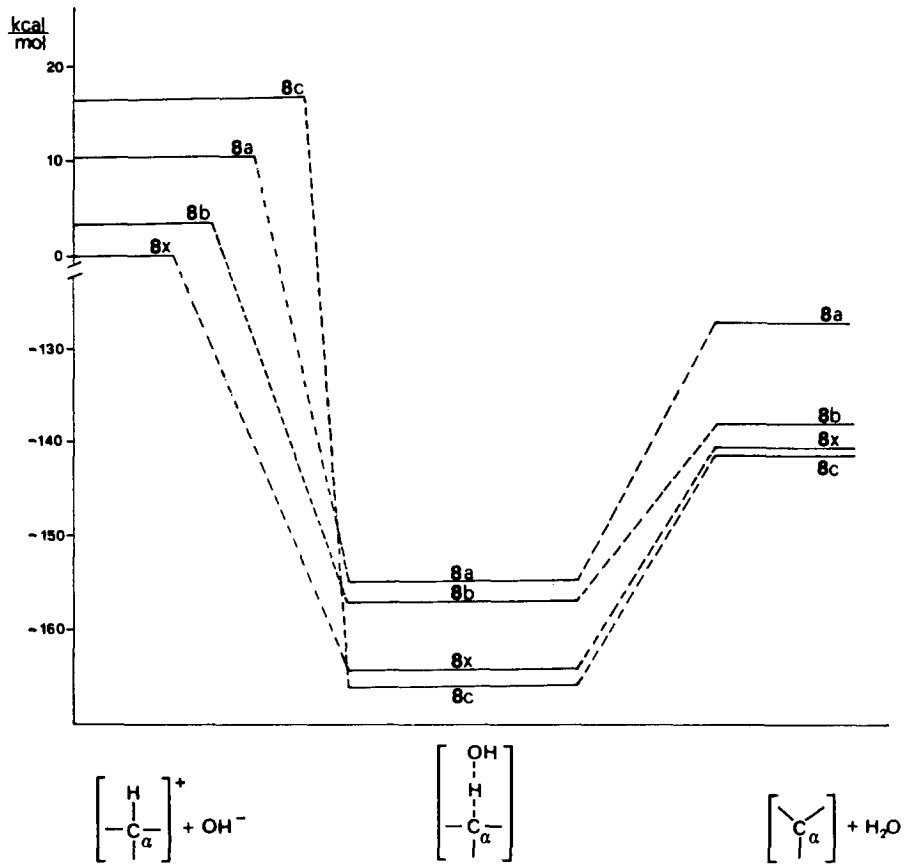

FIG. 6. Variation of energy in the formation of a molecular adduct among the conformational isomers **8a–8x** (protonated forms) and OH^-, and the subsequent proton abstraction from C_α to form the corresponding carbanion species. The zero of the energy scale is fixed to E(**8x**) + $E(OH^-)$.

ships in pyridoxal model systems. As is shown schematically in Fig. 6, the conformer **8c** containing a pseudoaxial C_α–H bond is the least favored energetically (by more than 16 kcal mol^{-1} with respect to the most stable chelate ring conformation). For this reason it has never been observed in the X-ray structural studies performed on metal chelates of type **3a** or **3b** and its abundance has been considered negligible in solution on the basis of CD investigations (*6–8*). In spite of its higher energy, conformer **8c** provides the most stable supermolecule generated by interaction with the approaching base and also the most stable carbanion species upon C_α–H proton detachment. The higher stability of the carbanion species derived from **8c** can be accounted for by considering that the pseudoequatorial arrangement of the amino acid side chain in **8c** is closest to the planar disposition in a trigonal planar carbanion. Some experimental support of these results comes from an NMR study of deuterium exchange by the methylene protons of a pyridoxylideneglycine–cobalt(III) complex (*30*). This showed a higher reactivity, i.e.,

easier C_α–H bond dissociation and/or higher carbanion stability, for the pseudoaxial proton with respect to the otherwise identical pseudoequatorial C_α–H proton. For any amino acid other than glycine, the C_α–H bond markedly prefers a pseudoequatorial orientation and this is quite certainly an important factor in determining the lower reactivity attainable by model systems of type **3a**, compared with the enzyme systems, in promoting the chemical process involving C_α–H bond cleavage.

In conclusion, the energy diagram in Fig. 6 provides theoretical support to Dunathan's hypothesis on the stereoelectronic requirements for easy cleavage of a bond to the amino acid α-carbon atom. Even though the absolute value of the energies involved in the various steps can be overestimated by the calculation method employed here, the trend observed is meaningful. The potential significance of the information obtained on model systems **8a–8c** for the enzyme systems comes from the observation that conformational orientation of the substrate–cofactor imine, forcing the amino acid residue in an unfavorable steric arrangement, e.g., with the C_α–H bond perpendicular to the plane of the conjugated imine, may not be a serious problem at the enzyme active site. Correct positioning of the groups on the polypeptide chain of the apoenzyme in the neighborhood of the substrate–cofactor complex can assist this process by appropriate interactions with the groups on the amino acid residue. For instance, simple considerations about the interaction of the carboxylate anion of the coenzyme–substrate complex with a positive site (R_3NH^+) of the protein show that the stabilizing energy can largely compensate the energy required to promote **8x** to **8c**, that is, to force the C_α–H bond in a pseudoaxial conformation. This interaction is of long-range nature and calculations on the acetate–methylammonium ion pair indicate that, even at a $RCOO^-$–NH_3R^+ distance of 2–10 Å the interaction energy is still of the order of 20–30 kcal mol^{-1}.

These data suggest that the lysyl amino group of the apoenzyme, which binds the cofactor in the absence of substrate but becomes free upon transimination (*31*), may play a role in the conformational orientation of the substrate–cofactor complex by locking the carboxyl group of the amino acid residue in a suitable position. In contrast, as discussed above, it is unlikely that such an amino group can act as the catalytic base in the C_α–H proton abstraction process.

REFERENCES

1. FOLKERS, K. (1986) *C & EN* **27**, 55.
2. BRAUNSTEIN, A. E. (1973) Enzymes 3rd ed., Vol. 9, p. 379; WALSH, C. (1979) Enzymatic Reaction Mechanisms, p. 777, Freeman, San Francisco; METZLER, D. E. (1979) *Adv. Enzymol.* **50**, 1.
3. MARTELL, A. E. (1982) *Adv. Enzymol.* **53**, 163.
4. DUNATHAN, H. C. (1971) *Adv. Enzymol.* **35**, 79; VEDERAS, J. C., AND FLOSS, H. G. (1980) *Acc. Chem. Res.* **13**, 455.
5. TSAI, M. D., BYRN, S. R. CHANG, C., FLOSS, H. G., AND WEINTRAUB, H. J. R. (1978) *Biochemistry* **17**, 3177.
6. CASELLA, L., AND GULLOTTI, M. (1983) *J. Amer. Chem. Soc.* **105**, 803.
7. SMITH, H. E. (1983) *Chem. Rev.* **83**, 359.

8. CASELLA, L., AND GULLOTTI, M. (1981) *J. Amer. Chem. Soc.* **103,** 6338; CASELLA, L., GULLOTTI, M., AND PACCHIONI, G. (1982) *J. Amer. Chem. Soc.* **104,** 2386; CASELLA, L., AND GULLOTTI, M. (1986) *Inorg. Chem.* **25,** 1293.
9. TSAI, M. D., WEINTRAUB, H. J. R., BYRN, S. R., CHANG, C., AND FLOSS, H. G. (1978) *Biochemistry* **17,** 3183.
10. TURMANYAN, V. G., MAMAEVA, O. K., BOCHAROV, A. L., IVANOV, V. I., KARPEISKY, M. Y., AND YAKOLEV, G. I. (1974) *Eur. J. Biochem.* **50,** 119.
11. DINER, S., MALRIEU, J. P., CLAVERIE, P., AND JORDAN, F. (1968) *Chem. Phys. Lett.* **2,** 319; DINER, S., MALRIEU, J. P., AND CLAVERIE, P. (1969) *Theor. Chim. Acta* **13,** 1; MALRIEU, J. P., CLAVERIE, P., AND DINER, S. (1969) *Theor. Chim. Acta* **13,** 18; DINER, S., MALRIEU, J. P., JORDAN, F., AND GILBERT, M. (1969) *Theor. Chim. Acta* **15,** 100; JORDAN, F., GILBERT, M., MALRIEU, J. P., AND PINCELLI, U. (1969) *Theor. Chim. Acta* **15,** 211.
12. POPLE, J. A., SANTRY, D. P., AND SEGAL, G. A. (1965) *J. Chem. Phys.* **43S,** 129; POPLE, J. A., AND SEGAL. G. A. (1965) *J. Chem. Phys.* **43S,** 136.
13. FANTUCCI, P., AND TOSI, C. (1981) XVI National Congress of the Italian Association of Chemical Physics, Abano Terme (Abstracts) p. 33.
14. CLAVERIE, P., DAUDEY, J. P., DINER, S., GIESSNER-PRETTRE, C., GILBERT, M., LANGLET, J., MALRIEU, J. P., PINCELLI, U., AND PULLMAN, B., QCPE program No. 220.
15. PRESS, W. H., FLANNERY, B. P., TEUKOLSKY, S. A., AND VETTERLING, W. T. (1986) *in* Numerical Recipes, p. 294, Cambridge Univ. Press, London/New York; POWELL, M. J. D., QCPE program No. 60.
16. ALLINGER, N. L. (1977) *J. Amer. Chem. Soc.* **99,** 8127.
17. COTTON, F. A., AND WILKINSON, G. (1972) *in* Advanced Inorganic Chemistry, p. 152, Wiley, New York, and references therein.
18. KORHONEN, K., AND HÄMÄLÄINEN, R., (1979) *Acta Chem. Scand. Ser. A* **33,** 569.
19. HÄMÄLÄINEN, R., AHLGREN, M., TURPEINEN, U., AND RANTALA, M. (1978) *Acta Chem. Scand. Ser. A* **32,** 235.
20. SUTTON, L. E. (1958) Tables of Interatomic Distances and Configurations in Molecules and Ions, Chem. Soc., London.
21. DUNATHAN, H. C. (1966) *Proc. Natl. Acad. Sci. USA* **55,** 713.
22. CHANG, C. C., LAGHAI, A., O'LEARY, M. H., AND FLOSS, H. G. (1982) *J. Biol. Chem.* **257,** 3564.
23. ASADA, Y., TANIZAWA, K., SAWADA, S., SUZUKI, T., MISONO, H., AND SODA, K. (1981) *Biochemistry* **20,** 6881.
24. TANIZAWA, K., YOSHIMURA, T., ASADA, Y., SAWADA, S., MISONO, H., AND SODA, K. (1982) *Biochemistry* **21,** 1104.
25. FEDERINK, C. S., AND SHAFER, J. A. (1983) *J. Biol. Chem.* **258,** 5372.
26. HOLM, R. H. (1973) *in* Inorganic Biochemistry (Eichhorn, G. L., Ed.), p. 1137. Elsevier, New York.
27. PASINI, A., AND CASELLA, L. (1974) *J. Inorg. Nucl. Chem.* **36,** 2133.
28. PHIPPS, D. A. (1979) *J. Mol. Catal.* **5,** 81.
29. METZLER, C. M., CAHILL, A., AND METZLER, D. E. (1980) *J. Amer. Chem. Soc.* **102,** 6075.
30. FISCHER, J. R., AND ABBOTT, E. H. (1979) *J. Amer. Chem. Soc.* **101,** 2781.
31. MAKELA, M. J., AND KORPELA, T. K. (1983) *Chem. Soc. Rev.* **12,** 309.